

Heterogeneous & Homogeneous & Bio- & Nano-

CHEM **CAT** CHEM

CATALYSIS

Accepted Article

Title: Kinetic Analysis of Catalytic Organic Reactions Using a Temperature Scanning Protocol

Authors: Olivia P. Schmidt, Anne-Marie Dechert-Schmitt, Michelle Garnsey, Hanna Wisniewska, and Donna Gail Blackmond

This manuscript has been accepted after peer review and appears as an Accepted Article online prior to editing, proofing, and formal publication of the final Version of Record (VoR). This work is currently citable by using the Digital Object Identifier (DOI) given below. The VoR will be published online in Early View as soon as possible and may be different to this Accepted Article as a result of editing. Readers should obtain the VoR from the journal website shown below when it is published to ensure accuracy of information. The authors are responsible for the content of this Accepted Article.

To be cited as: *ChemCatChem* 10.1002/cctc.201900560

Link to VoR: <http://dx.doi.org/10.1002/cctc.201900560>

WILEY-VCH

www.chemcatchem.org



COMMUNICATION

Kinetic Analysis of Catalytic Organic Reactions Using a Temperature Scanning Protocol

Olivia P. Schmidt,^[a] Anne-Marie Dechert-Schmitt,^{[b]*} Michelle R. Garnsey,^[b] Hanna M. Wisniewska,^[b] and Donna G. Blackmond^{*[a]}

Dedicated to the memory of Miss Maud Leonora Menten on the 140th anniversary of her birth.

Abstract: Experimental and kinetic modelling studies are presented to describe the development of temperature scanning reaction progress protocol for batch reactions. Coupled with graphical manipulations, this approach enables the expansion of in-situ kinetic studies from a focus on isothermal concentration profiles to include reaction temperature as a parameter for rapid kinetic and mechanistic analysis.

In-situ monitoring of reaction progress has become a standard tool in mechanistic analysis of catalytic organic reactions both in academia and in the pharmaceutical industry. The ability to obtain a real-time concentration scan spanning the full conversion regime led to the development of Reaction Progress Kinetic Analysis (RPKA),^{[1],[2]} a methodology combining accurate monitoring of temporal reaction progress with innovative graphical approaches to interpreting data from batch reactions. Using RPKA, extensive information content is obtained from a smaller number of separate experiments than are required in classical kinetic approaches. RPKA allows evaluation of concentration dependences and catalyst robustness, and this information may then be used to develop a reaction mechanism, to construct a reaction rate expression, to streamline batch process optimization, or to design an efficient flow process.

Such temporal concentration scans obviate the need for discrete “initial rate” measurements that employ reaction conditions that are often far from synthetically relevant, require extensive effort in time, and ultimately discard significant amounts of data. In a vein similar to RPKA, one might envision the development of continuous means of measuring reaction variables other than concentrations. One such key variable is reaction temperature. Although probing the influence of temperature is important in pharmaceutical process safety protocols such as adiabatic reaction calorimetry, early studies in this area^[3] have not to date resulted in the adoption of an approach analogous to RPKA for systematically scanning temperature as a reaction variable in complex organic catalytic reactions. Typically, separate isothermal reactions are carried out at a number of different temperatures to develop an Arrhenius relationship for the observed rate constants in liquid or multi-phase reactions.

The development of an approach that provides a temporal scan of temperature during reaction progress would represent a significant tool for increasing the efficiency of mechanistic analysis. Such a tool was introduced in the form of a temperature scanning reactor (TSR) more than twenty years ago by Wojciechowski,^[4] primarily for studying gas phase flow reactions in the petrochemical industry. Those studies lacked the powerful in-situ reaction monitoring tools that are now state-of-the-art in batch organic catalytic reaction studies, and the TSR methodology required an extensive number of separate experiments. Landau et al. used a temperature-step protocol to optimize both temperature and reagent delivery in liquid-phase batch and semi-batch reactions that incorporated continuous heat flow kinetic measurements.^[5] More recently, Jensen has further developed a temperature scanning approach for flow reactors that exploits continuous spectroscopic monitoring where temperature and space velocity are changed simultaneously.^[6] Gavriilidis and coworkers have further developed this approach into an autonomous microreactor platform for rapid identification of kinetic models.^[7] A comparison of batch and ideal plug flow reactors equates distance or space velocity in flow with reaction time in batch. While great strides have been made in the past decade in the development of detailed, quantitative kinetic analysis in continuous flow reactor operation,^{[8],[9]} issues may still arise from unsteady-state behavior due to changing flow rates. It has been noted that kinetic measurements carried out in batch offer a streamlined approach to reaction design and optimization for reactions ultimately carried out under either batch or flow operation.^[10]

The work presented herein expands on the concept of continuous temperature change for liquid-phase catalytic organic reactions carried out in a laboratory flask or a batch reactor incorporating in-situ monitoring tools. Experimental data and kinetic modelling studies demonstrate how this approach may aid in mechanistic analysis. Our approach involves carrying out a reaction while ramping reaction temperature in a controlled fashion while simultaneously monitoring reaction progress. As an example, Figure 1 shows a model plot of a reaction in which rate and substrate concentration are plotted as a function of time during a reaction carried out using a linear temperature ramp. Temporal reaction rate may be calculated from the measured concentration profile, or vice versa. Each time point thus represents a separate measurement of reaction rate at a specific substrate concentration and a specific temperature. With these data, predictive modeling may be carried out to estimate reaction rate expressions and activation parameters, to test mechanistic hypotheses, and to develop optimal reaction conditions.

[a] Dr. O. Schmidt, Prof. Dr. D.G. Blackmond
Department of Chemistry
The Scripps Research Institute
La Jolla, CA 92037 USA
E-mail: blackmond@scripps.edu

[b] Dr. A.-M. Dechert-Schmitt, Dr. M.R. Garnsey, Dr. H.M. Wisniewska
Pfizer Worldwide Research and Development
Groton CT, 06340 USA

COMMUNICATION

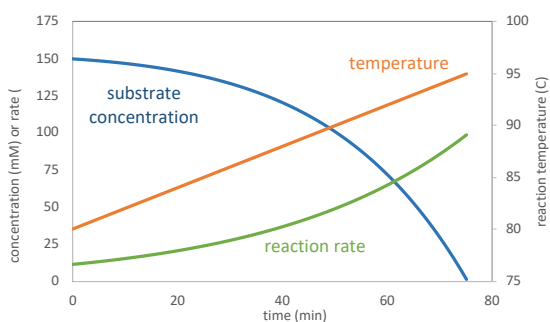
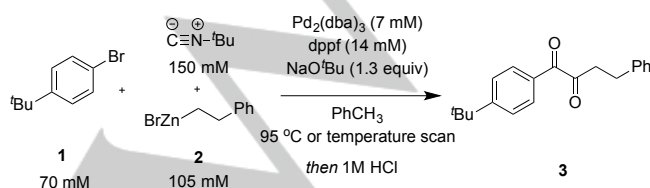


Figure 1. Illustration of temporal profiles of reaction rate, substrate concentration, and reaction temperature for a reaction carried out using a temperature scanning protocol of 0.2 °C/min.

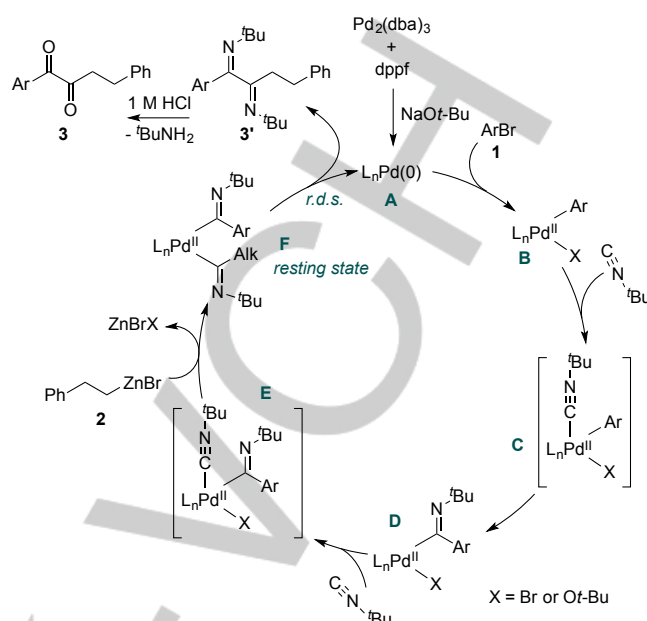
The temperature scanning profile may serve as a fingerprint of the form of the reaction rate expression. For a general reaction $A + B \rightarrow P$, the rate expression will be of the form shown in Eq. (1), where the rate constant is a function of temperature, and the change in substrate concentrations can be a function of both temperature and reaction time. A successful temperature scanning protocol must allow deconvolution of the effects of concentration and temperature on reaction rate.

$$\text{rate} = k(T) \cdot f([A](T, t)) \cdot f([B](T, t)) \quad (1)$$

In order to demonstrate this temperature scanning protocol, we chose to study the multi-component Pd-catalyzed synthesis of diketones shown in Scheme 1 that employs ^tBu isocyanide as a CO equivalent.^{[11],[12]} Our previous kinetic and mechanistic study of this reaction system proposed the reaction mechanism shown in Scheme 2. We proposed that oxidative addition of an aryl bromide **1** to the Pd/dppf catalyst is followed by double insertion of the isocyanide and transmetalation of an alkylzinc bromide **2**. Rate-determining reductive elimination gives the product diimine, which yields the diketone **3** upon acidic workup. The diketone products may be elaborated further to medicinally important heterocycles such as quinoxaline derivatives. The reaction rate and rate-determining step may be influenced by bite angle of the bidentate phosphine ligand employed, in accordance with previous studies demonstrating ligand effects on both rate and selectivity in reactions catalyzed by transition metals with bidentate phosphine ligands. The rate of oxidative addition is observed to increase with ligands of smaller bite angles, while the rate of reductive elimination increases using ligands of larger bite angles.^[13] The change in rate-determining step results in a change in the reaction order in substrate concentrations.



Scheme 1. Pd-catalyzed synthesis of diketones.^[4]



Scheme 2. Proposed mechanism for the reaction of Scheme 1.

We monitored the reaction of Scheme 1 using ReactIR spectroscopy by following the isocyanide peak at 2133 cm^{-1} . Validation by GC analysis of discrete reaction aliquots allowed calculation of all other components from the reaction stoichiometry and mass balance.^[11] Figure 2a (orange symbols) shows a product profile monitored under isothermal conditions. The reaction exhibits a constant rate revealing overall zero-order kinetics, in accordance with the mechanistic proposal of Scheme 2 with reductive elimination of the product as the rate-determining step.

We then carried out the reaction of Scheme 1 using a linear temperature ramp between 80–100 °C at 0.2 °C/min, as is also shown in Figure 2a. Under temperature scanning conditions, the reaction commences more slowly at lower temperature but then accelerates rapidly as reaction temperature increases. A comparison of the calculated temporal rate profiles for the two sets of conditions is shown in Figure 2b.

Manipulation of the zero-order kinetic data in this reaction offers the opportunity to evaluate temperature dependence in a straightforward manner from a single experiment. Because reaction rate does not depend on reactant concentration in this case, the temperature-dependent rate constant over the course of the temperature scanning profile may be evaluated without the need to account for changes in concentration driving forces. Eq. (2) shows that the exponential dependence on temperature, T , that is expected for zero-order kinetics (A_{pre} = pre-exponential factor, with units of rate; E_{act} = activation energy in kJ/mol; R = ideal gas constant = 0.008314 kJ/mol·K).

COMMUNICATION

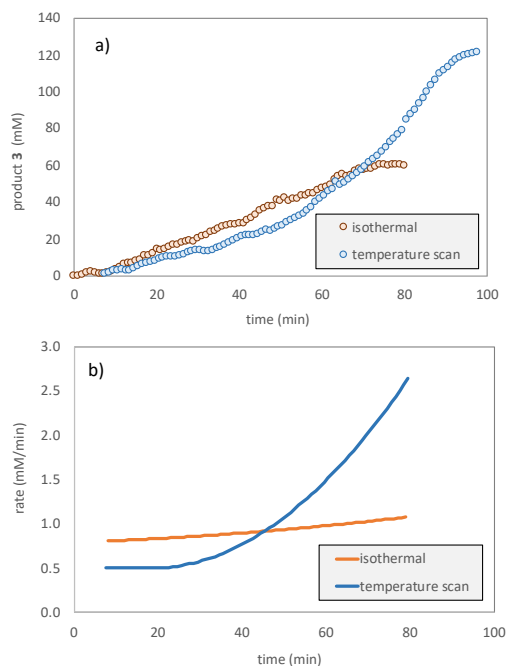


Figure 2. (a) Concentration profiles for the reaction of Scheme 1 monitored by ReactIR spectroscopy. Orange symbols: isothermal reaction as in Scheme 1; Blue symbols: temperature scanning reaction from 80-100 °C at 0.2 °C/min (conditions as in Scheme 1 with two-fold reactant concentrations); b) Temporal reaction rate profiles calculated from the concentration data in (a).

$$\text{rate}(0^{\text{th}} \text{ order}) = k = A_{\text{pre}} \cdot \exp\left(\frac{-E_{\text{act}}}{RT}\right) \quad (2)$$

Figure 3 shows that a plot of $\ln(\text{rate})$ vs. $1/T$ derived from the temperature scan reaction of Figure 2 yields a linear relationship over the course of the reaction. In this case, the exponential relationship shown in Eq. (2) is demonstrated with a single temperature scanning profile. An activation energy of ca. 171 kJ/mol is obtained from the slope of this curve. In conventional kinetic analysis, an evaluation of temperature dependence as shown in Figure 3 would typically require rate measurements from multiple separate isothermal reactions. The simple case shown here of zero-order kinetics in substrate concentrations demonstrates how this temperature scanning reaction protocol can provide a streamlined approach to predicting the temperature dependence of reaction rate.

Kinetic modelling of different scenarios may be carried out to illustrate the extension of this protocol to reactions exhibiting other than zero-order dependence on substrate concentrations. We first consider the case of a reaction that exhibits overall first-order kinetics under isothermal conditions. As mentioned previously, first order kinetics may be observed in the reaction of Scheme 1 out using catalysts with bidentate phosphine ligands of smaller bite angles, where oxidative addition of ArBr becomes rate-determining in the mechanism shown in Scheme 2. Eq. (3) shows the temperature dependence for first-order kinetics in a reaction where $[A]_0$ = initial concentration of substrate **A**. Over the course of the temperature scanning reaction, rate decreases as substrate concentration decreases, but increases as temperature increases,

meaning the two effects oppose each other in a temperature scanning protocol.

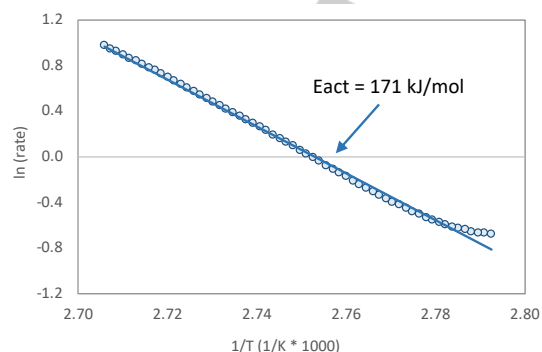


Figure 3. Arrhenius plot of the temperature scanning reaction profile from Figures 1 and 2.

$$\begin{aligned} \text{rate}(1^{\text{st}} \text{ order}) &= k \cdot [A] = k \cdot [A]_0 \cdot \exp(-kt) \\ &= A_{\text{pre}} \cdot \exp\left(\frac{-E_{\text{act}}}{RT}\right) \cdot [A]_0 \cdot \exp\left(-A_{\text{pre}} \cdot \exp\left(\frac{-E_{\text{act}}}{RT}\right) \cdot t\right) \end{aligned} \quad (3)$$

Figure 4 shows results from simulation of a first order reaction carried out using a linear temperature scan rate of 0.2 °C/min. The opposing influences of rate constant and substrate concentration on the reaction rate are evident, with the rate initially increasing with increasing temperature and then ultimately decreasing as the substrate driving force is expended over the course of the temperature scanning reaction.

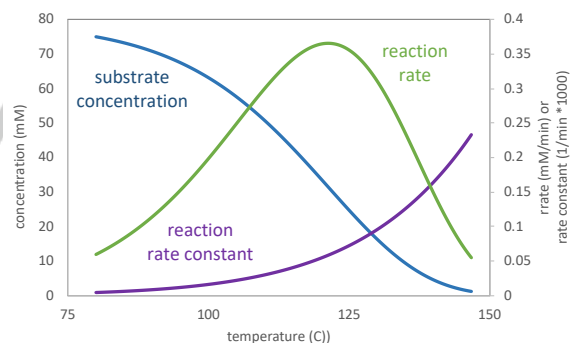


Figure 4. Kinetic profiles plotted vs. temperature for a simulated first-order reaction carried out at a linear temperature scanning rate of 0.2 °C/min. Simulation parameters are $E_{\text{act}} = 75$ kJ/mol and $A_{\text{pre}} = 1 \times 10^8$ min⁻¹.

For this case of first order kinetics, the temperature-dependent rate constant may be obtained simply by dividing the reaction rate by the substrate concentration at each time point representing a unique temperature, as shown in Eq. (4).

$$\frac{\text{rate}(1^{\text{st}} \text{ order})_T}{[A]_T} = k_T \quad (4)$$

COMMUNICATION

The resulting rate constant profile (shown in purple in Figure 4) reveals the expected exponential behavior and yields a straight line when plotted as $\ln k$ vs. $1/T$ (Figure 5, purple line).

A key point that is often overlooked when probing temperature effects via separate isothermal experimental measurements is that rate measurements must be carried out over the same concentration interval – not necessarily the same time interval – for each reaction at a different temperature. This is because a reaction may proceed to a much higher conversion at higher temperature over the same time interval as a reaction carried out at lower temperature. For isothermal reaction data in cases where the rate law, and thus the rate constant, may not be known a priori, Arrhenius plots are often constructed simply by plotting the observed rate, or k_{obs} vs $1/T$. Such a plot may potentially convolute the (typically opposing) effects of temperature and concentration on reaction rate. Figure 5 demonstrates this for the model first order reaction, showing that a plot (green line) of $\ln(\text{rate})$ vs. $1/T$ yields, instead of straight line, a curve of unusual shape that may even predict negative activation energies over part of the temperature range. The temperature scanning protocol using Eq. (4) normalizes the rate by concentration and allows the temperature dependence of rate measured in the temperature scanning reaction to be deconvoluted from the reactant concentration dependence in this plot.

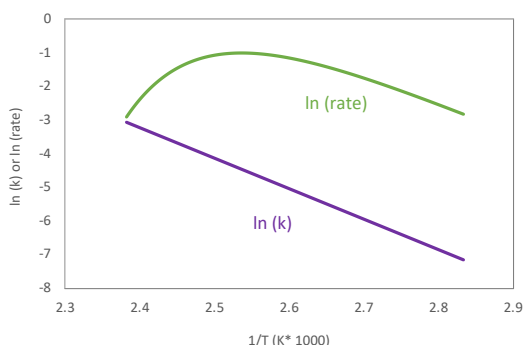


Figure 5. Arrhenius plots from the model reaction simulation of Figure 4, plotted as $\ln k$ in purple and $\ln(\text{rate})$ in green.

The results of the simulations in Figure 5 reveal that simple data manipulations permit deconvolution of the influences of concentrations and temperature on reaction rate. For this case of first-order kinetics, an in-situ experimental probe that allows temporal measurement of both rate and concentration (or measurement of one variable and calculation of the other from this measurement) is all that is required to obtain a quantitative analysis of the reaction's temperature dependence from a single temperature scanning reaction.

Although analysis of temperature scanning data can become more complex when reactions other than simple zero- or first-order kinetics are under study, judicious data manipulation may still provide the means to deconvolute competing influences and provide valuable mechanistic information. For example, catalytic reactions that exhibit saturation kinetics involve a shift in the cycle's rate-determining step from high to low substrate concentrations. In simple Michaelis-Menten^[14] kinetics, this is manifested as a change in reaction order from 0th to 1st order from

high concentration to low substrate concentration. The Michaelis-Menten rate expression, *rate* (MM), shown in Eq. (5) describes a reaction where catalyst binds to substrate **A** with an equilibrium constant $K_{eq,A}$ and then reacts in a rate-determining step with rate constant k_{rds} . At high substrate concentrations or strong substrate binding ($K_{eq,A}[\mathbf{A}] \gg 1$), reaction rate will be proportional to k_{rds} , while at low substrate concentrations ($K_{eq,A}[\mathbf{A}] \ll 1$), rate will be proportional to the quantity $k_{rds} \cdot K_{eq,A}$. The elementary kinetic rate constant and the binding equilibrium constant may each exhibit their own temperature dependence, and these may be deconvoluted by examining the limiting cases. Comparing plots of rate vs. time and rate/[**A**] vs. time and looking for linear regions and shifts in the slope may also provide clues about the conditions under which a shift in rate-determining step occurs.

$$\text{rate}(MM) = \frac{k_{rds} K_{eq,A} [\mathbf{A}]}{1 + K_{eq,A} [\mathbf{A}]} \quad (5)$$

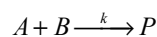
$$\text{at high } K_{eq,A} [\mathbf{A}]: \quad \text{rate}(MM) = k_{rds}$$

$$\text{at low } K_{eq,A} [\mathbf{A}]: \quad \text{rate}(MM) = k_{rds} K_{eq,A} [\mathbf{A}]$$

Michaelis-Menten kinetic profiles may be approximated over a given range of concentrations by a power-law form of the rate expression, $\text{rate} = k' \cdot [\mathbf{A}]^x$ (Eq. (6)), with the value of "x" falling between 0 and 1, and its magnitude providing clues about the binding strength. In a generalization of the normalization operation of Eq. (4), the experimental rate curve from a temperature scanning reaction following Michaelis-Menten kinetics may be divided by the experimental concentration data raised to some power "x" to give the rate constant profile. The value of "x" that best describes the reaction under study is the value that yields a straight line in an Arrhenius plot of $\ln k'$ vs. $1/T$.

$$\text{rate}_T = k'_T [\mathbf{A}]_T^x ; \quad \frac{\text{rate}_T}{[\mathbf{A}]_T^x} = k'_T \quad (6)$$

For reactions with concentration dependences on more than one substrate, the relationship between substrate concentrations is determined by the reaction stoichiometry. Using the concept of "excess" ($[xs] = [\mathbf{B}]_0 - [\mathbf{A}]_0$), a rate law containing only one distinct concentration variable may be constructed as in Eq. (7), and normalization procedures analogous to those discussed above may be carried out to extract a temperature-dependent power law rate constant.



$$\text{rate} = k \cdot [\mathbf{A}]^m \cdot [\mathbf{B}]^n = k \cdot [\mathbf{A}]^m \cdot [\mathbf{A} + xs]^n \quad (7)$$

$$\frac{\text{rate}}{[\mathbf{A}]^m \cdot [\mathbf{A} + xs]^n} = k$$

Kinetic modelling of such an example is shown in Figure 6, for the case of an organocatalytic aldol reaction studied previously

COMMUNICATION

under isothermal conditions.^[15] The rate constant curve is obtained from Eq. (7) with $m = 0.58$ and $n = 0.9$. Plots of $\ln(k)$ vs. $1/T$ for Eq. (7) with these values of m and n as well as other values are shown in Figure 7. When values of m and n are not correctly chosen, curvature appears in the plots. Temperature scanning experiments to confirm the temperature scanning model for this reaction are ongoing.

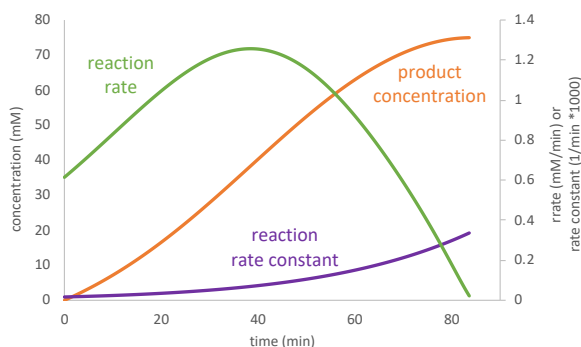


Figure 6. Kinetic profiles plotted vs. time for a simulated non-integral order reaction as in Eq. (7) carried out at a linear temperature scanning rate of 0.4 °C/min. $[A]_0 = 75$ mM, $[B]_0 = 100$ mM, $[X]_0 = 0.25$ mM, $T_0 = 80$ °C. Simulation parameters are $E_{act} = 75$ kJ/mol and $A_{pre} = 1 \times 10^8$ min⁻¹.

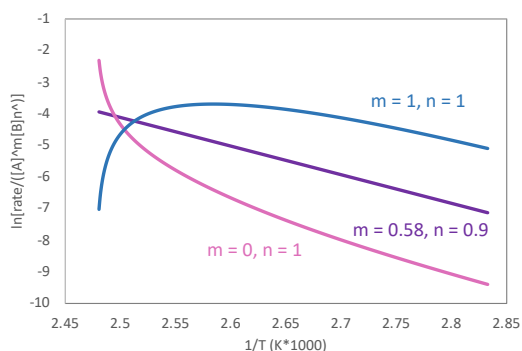


Figure 7. Arrhenius plots from the model reaction simulation of Figure 6, plotted as $\ln(k)$ from Eq. (7) for $m=0.58$, $n=0.9$ (purple); $m=1$, $n=1$ (blue); $m=0$, $n=1$ (pink).

In summary, we report experimental data manipulations and kinetic simulations describing a novel temperature scanning protocol that may be used in combination with in-situ reaction monitoring and reaction progress kinetic analysis to probe the temperature dependence of organic catalytic reactions. The protocol may be applied in rapid screening of new reactions, in fundamental mechanistic analysis, and in reaction optimization aimed at scale-up for commercial manufacturing. An understanding of the influence of temperature on the reaction may thus be obtained in far fewer separate experiments than have traditionally been required under isothermal operation, thus streamlining both process research and mechanistic studies of organic catalytic reactions.

Experimental Section

All compound characterization data is available in Ref. [4], as well as detailed experimental procedures for reactions using isothermal ReactIR spectroscopic measurements and GC calibration. For the temperature scanning reaction, $\text{Pd}_2(\text{dba})_3$ (25.6 mg, 0.028 mmol), dppf (31.0 mg, 0.056 mmol), and 2,6-dimethoxytoluene (Int. Std.; 54.4 mg, 0.357 mol) were added to an oven-dried 16 ml borosilicate glass mixing vessel equipped with a stir bar. The reaction vessel was fitted to the ReactIR probe through a PTFE septa with the probe aligned just above the stir bar. The reaction vessel was evacuated and refilled with argon three times through the PTFE septa. Toluene (1.73 ml), *tert*-butylisocyanide (136 μl , 100 mg, 1.20 mmol), and 1-bromo-4-*tert*-butylbenzene (97.1 μl , 119 mg, 0.56 mmol) were added. After stirring at room temperature for 5 min, NaOt-Bu (2 M in THF, 360 μl , 0.72 mmol) and phenylethyl zinc bromide (0.5 M in THF, 1.68 ml, 0.84 mmol) were added and the reaction mixture was placed into an Omnical SuperCRC reaction microcalorimeter (used as a temperature controller) at 82 °C. The reaction mixture was equilibrated at 82 °C for 25 min and the temperature ramp was started with a ramp rate of 0.2 °C / min. After completion of the reaction, 0.3 ml of the reaction mixture was diluted into 1 ml of toluene. The solution was concentrated in vacuo and THF (0.2 ml) and HCl (1 M, 0.2 ml) were added. After 1 h, an aliquot of this solution (50 μl) was diluted into MeOH (1 ml) for GC analysis.

Experimental ReactIR concentration profiles were smoothed using a moving average and fit to a function (e.g., a series of polynomials) in order to calculate a noise-free reaction rate profile from the mathematical derivative of the concentration profile. First-order kinetic reaction simulations shown in Figures 4 and 5 were completed in Excel using Eqs. 3 and 4. Rate constants were simulated as a function of temperature and time for a given temperature ramp rate. The initial rate at the initial temperature value is given by $r_0 = k_{T_0} [A]_0$. Subsequent concentrations at subsequent time (temperature) points were calculated from the previous rate and $[A]$ values, as: $[A]_1 = [A]_0 - r_0(t_1 - t_0)$. Rate at each time (temperature) point is calculated as: $r_{T_i} = k_{T_i} [A]_{T_i}$.

Acknowledgements

D.G.B. acknowledges personal communications with B.W. Wojciechowski. O.P.S. acknowledges funding from the SNSF. A previous isothermal experiment conducted by J.I. Murray is acknowledged.

Keywords: kinetics • temperature scan • Pd catalysis • Michaelis-Menten kinetics • Arrhenius plot

- [1] a) D.G. Blackmond, *Angew. Chemie Int. Ed.* **2005**, *44*, 4032–4320; b) J.S. Mathew, M. Klussmann, H. Iwamura, F. Valera, A. Futran, E.A.C. Emanuelsson, D.G. Blackmond, *J. Org. Chem.* **2006**, *71*, 4711–4722; c) D.G. Blackmond, *J. Am. Chem. Soc.* **2015**, *137*, 10852–10866.
- [2] J. Burés, Bures, *Angew. Chem. Int. Ed.* **2016**, *55*, 16084–16087.
- [3] a) W. Frankvoort, W.R. Dammers, *Thermochim. Acta* **1975**, *11*, 5–16; b) Y.-S. Duh, C.-C. Hsu, C.-S. Kao, S.W. Yu, *Thermochim. Acta* **1996**, *285*, 67–79.
- [4] a) B. W. Wojciechowski, *Chem. Eng. Comm.* **2003**, *190*: 1115–1131; b) Patent US5593892 – Temperature scanning reactor method (Inventors: Bohdan W. Wojciechowski, Norman Rice), Jan. 14, 1997.
- [5] R.N.Landau, D.G. Blackmond, H.-H.Tung, *Ind. Eng. Chem. Res.* **1994**, *33*, 814–820.
- [6] K.C. Aroh, K.F. Jensen. *React. Chem. Eng.* **2018**, *3*, 94–101.
- [7] C. Waldron, A. Panakajakshan, M. Quaglio, E. Cao, F. Galvanin, A. Gavriilidis. *React. Chem. Eng.* **2019**, <https://doi.org/10.1039/C8RE00345A>.

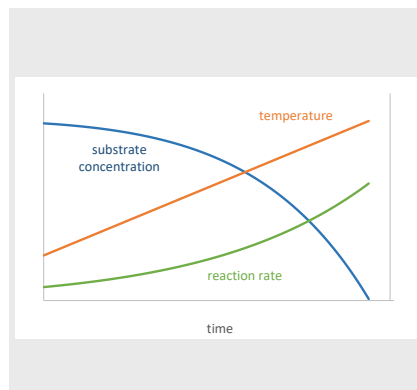
COMMUNICATION

- [8] a) P. J. Nieuwland, R. Segers, K. Koch, J. C. M. van Hest, F.P.J.T. Rutjes, *Org. Process Res. Dev.* **2011**, *15*, 783–787; b) J.P. McMullen, K. F. Jensen, *Org. Process Res. Dev.* **2011**, *15*, 398–407; c) B.J. Reizman, K.F. Jensen, *Org. Process Res. Dev.* **2012**, *16*, 1770–1782.
- [9] a) S. Mozharov, A. Nordon, D. Littlejohn, C. Wiles, P. Watts, P. Dallin, J.M. Girkin, *J. Am. Chem. Soc.* **2011**, *133*, 3601–3608; b) J. S. Moore K.F. Jensen, *Angew. Chem., Int. Ed.* **2014**, *53*, 470–473; c) S. Schwolow, F. Braun, M. Rädle, N. Kockmann, T. Röder, *Org. Process Res. Dev.* **2015**, *19*, 1286–1292; d) C. A. Hone, N. Holmes, G. R. Akien, R.A. Bourne, F.L. Muller, *React. Chem. Eng.* **2017**, *2*, 103–108; e) J.S. Moore, C.D. Smith and K.F. Jensen, *React. Chem. Eng.* **2016**, *1*, 272–279.
- [10] D.G. Blackmond, *Angew. Chemie. Int. Ed.* **2010**, *49*, 2478–2485.
- [11] A.-M. Dechert-Schmitt, M.R. Garnsey, H.M. Wisniewska, J.I. Murray, T.Lee, D.W. Kung, N. Sach, D.G. Blackmond, *ACS Catalysis* **2019**, *9*, 4508–4515.
- [12] a) T. Vlaar, E. Ruijter, B.U.W. Maes, R.V.A. Orru, *Angew. Chem. Int. Ed.* **2013**, *52*, 7084–7097; b) V.P. Boyarskiy, N.A. Bokach, K.V. Luzyanin, V.Y. Kukushkin, *Chem. Rev.* **2015**, *115*, 2698.
- [13] P. Dierkes, P.W.N.M. van Leeuwen, *JCS Dalton Trans.* **1999**, 1519–1529.
- [14] L. Michaelis, M.L. Menten, *Biochem. Z.* **1913**, *49*, 333–369.
- [15] N. Zotova, L.J. Broadbelt, A. Armstrong, D.G. Blackmond, *Bioorg. Med. Chem. Lett.* **2009**, *19*, 3934–3937.

COMMUNICATION

COMMUNICATION

A temperature scanning protocol coupled with reaction progress kinetic analysis helps to streamline mechanistic and process optimization studies to include the influence of temperature on organic catalytic reactions.



Olivia P. Schmidt,^[a] Anne-Marie Dechert-Schmitt,^[b]* Michelle R. Garnsey,^[b] Hanna M. Wisniewska,^[b] and Donna G. Blackmond^{*[a]}

Page No. – Page No.

Kinetic Analysis of Catalytic Organic Reactions Using a Temperature Scanning Protocol

Accepted Manuscript